Bulgarian Chemical Communications, Volume 48, Special Issue A (pp. 95 - 100) 2016

Effect of the synthesis procedure on the electrochemical properties of $Na_{2/3}Ni_{1/2}Mn_{1/2}O_2$ used as an electrode material in lithium-ion batteries

M. Kalapsazova*, R. Stoyanova, E. Zhecheva

Institute of General and Inorganic Chemistry, Bulgarian Academy of Sciences, Acad. G. Bonchev Str., Bldg. 11, Sofia 1113, Bulgaria

Submitted on July 20, 2015; Revised on October 23, 2015

Abstract. In this contribution, we study in details the effect of synthesis procedure on the electrochemical properties of $Na_xNi_{1/2}Mn_{1/2}O_2$ with x=2/3 when it is used as an electrode in lithium cells. For the preparation of oxides $Na_{0.67}Ni_{0.5}Mn_{0.5}O_2$, the precursor-based method was chosen. The method of synthesis is based on the formation of homogeneous precursor phases, which are easily transformed to the target product by a sequence of low-temperature reactions. The precursors are obtained by freeze-drying of aqueous solutions of Li(I), Ni(II) and Mn(II) salts. Two types of soluble salts are selected: acetate and nitrates. Thermal treatment of freeze-dried acetate-nitrate precursors at temperatures above 400 ºC yields layered $Na_{0.67}Ni_{0.5}Mn_{0.5}O_2$ with a *P*3-type of structure. Thermal properties of acetate-nitrate precursors are studied by DTA/TG analysis. The crystal structure and morphology of $Na_xNi_{1/2}Mn_{1/2}O_2$ are analyzed by means of X-ray powder diffraction and SEM analysis. The electrochemical properties of $Na_{0.67}Ni_{0.5}Mn_{0.5}O_2$ are examined in model lithium cells. The oxide $Na_{0.67}Ni_{0.5}Mn_{0.5}O_2$ obtained from freeze-dried acetate precursors displays a better electrochemical performance in terms of reversible capacity and cycling stability.

Keywords: Sodium deficient transition metal oxides; Layered oxides; Intercalation; Lithium-ion battery

1.INTRODUCTION

Searching for high-power electrode materials for lithium ion batteries, lithium transition metal oxides with a layered structure have been identified as the most suitable compounds [1,2]. Because of the two-dimensiponal Li diffusion, the electrochemical performances of oxides critically depend on the method of synthesis [1,2]. Two main types of synthetic procedures are developed during the last years [3,4]. The first one aims to stabilize the layered structure of delithiated oxides by rational metal substitutttion for electrochemically active ions [3], the second type of procedure is directed to design the morphology of oxides in order to make the Li diffusion more easy [4].

Recently, we reported a new concept for design of electrode materials. The concept is aimed at using directly new structure modification of sodium deficient nickel-manganese oxides $Na_xNi_{0.5}Mn_{0.5}O_2$ (x=0.50 and 0.67) as electrode materials instead of lithium analogues [5,6]. The advantage of using $Na_xNi_{0.5}Mn_{0.5}O_2$ is based on their larger interlayer space, which is beneficial both for a rapid exchange of Na^+ with Li^+ and for an easier lithium diffusion. The electrochemical intercalation of Li^+ into layered $Na_xNi_{0.5}Mn_{0.5}O_2$ takes place at 3.04 V and leads to a structural transformation from the *P3*- to the *O3*-type of structure [7]. The *in-situ* generated *O3*-phase containing simultaneously lithium and sodium determines the further electrochemical response of $Na_xNi_{0.5}Mn_{0.5}O_2$ in terms of voltage profile, cycling stability and rate capability. Our findings reveal the unique ability of the new structure modification of $Na_xNi_{0.5}Mn_{0.5}O_2$ (i.e. *P*3-type of structure) for application as low-cost electrode materials in lithium ion batteries.

In this contribution, we extend our studies by exploring the effect of the synthesis procedure on the electrochemical properties of $Na_xNi_{1/2}Mn_{1/2}O_2$ with x=2/3 when it is used as an electrode in lithium cells. For the preparation of oxides $Na_xNi_{1/2}Mn_{1/2}O_2$, the precursor-based method was chosen. The method of synthesis is based on the formation of homogeneous precursor phases, which are easily transformed to the target product by a sequence of low-temperature reactions. The precursor-based procedure is a powerful tool for the formation of electrode materials with well defined structure and morphology [8,9]. In this study, the precursor phases are obtained by freeze-drying of aqueous solutions of Li(I), Ni(II) and Mn(II) salts. Two types of soluble salts are used: acetate and nitrates. The advantage of this method is related with the ability to control the extent of mixing of Li(I), Ni(II) and Mn(II) ions in the solid precursor phases. Thermal treatment of acetate-nitrate precursors at temperatures above 400 ºC yields $Na_xNi_{1/2}Mn_{1/2}O_2$ products. Thermal properties of acetate-nitrate precursors are studied by DTA/TG analysis. The crystal structure and morphology of

*To whom all correspondence should be sent:
E-mail: maria_l_k@svr.igic.bas.bg

$Na_xNi_{1/2}Mn_{1/2}O_2$ is analyzed by means of X-ray powder diffraction and SEM analysis. The electrochemical properties of $Na_xNi_{1/2}Mn_{1/2}O_2$ are examined in model lithium cells.

2.EXPERIMENTAL

Sodium-nickel-manganese oxides are prepared from freeze-dried acetate precursors. The procedure of the preparation is given elsewhere [5,6]. The homogeneous acetate precursors were prepared by freeze-drying of the corresponding Na, Ni and Mn acetate solutions (0.5 M). The nominal Na-to-(Mn+Ni) ratio was 0.67. The freeze-drying process was performed with an Alpha-Crist Freeze-Dryer at -20 °C in vacuum. The freeze-dried acetate precursors are decomposed at 400 °C in O_2 atmosphere for 3 hours. After thermal decomposition of the precursors, the solid residue was homogenized, pelleted and annealed at 700 °C in air for 24 hours, followed by cooling down to room temperature.

The same procedure is applied for the preparation of $Na_xNi_{1/2}Mn_{1/2}O_2$ from mixed nitrate-acetate precursors, where nickel nitrate is used instead of nickel acetate. For the sake of convenience, $Na_{0.67}Ni_{0.5}Mn_{0.5}O_2$ obtained from acetate and mixed nitrate-acetate precursors will be denoted further by NNM-Ac and NNM-NAc.

The thermal analysis (simultaneously obtained DTA-, TG-, DTG-, and evolved gas curves) of the freeze-dried precursors was carried out by a combined LABSYS^{TM} EVO DTA/TG system of the SETARAM Company, France, with a gas-analyser of the OmniStar™ type. The samples are investigated at a heating rate of 10 °C/min in O_2 flow (20 ml/min).

The X-ray structural analysis was made by a Bruker Advance 8 diffractometer with LynxEye detector using CuKα radiation. Step-scan recordings for structure refinement by the Rietveld method are carried out using 0.02° 2θ steps of 4 s duration. The diffractometer zero point, the Lorentzian/Gaussian fraction of the pseudo-Voigt peak function, the scale factor, the unit cell parameters, the thermal factors and the line half-width parameters were determined. The computer FullProf Suite Program (1.00) was used in the calculations [10].

The morphology of the precursors and target products is observed by JEOL JSM 6390 scanning electron microscope equipped with an energy dispersive X-ray spectroscopy (EDS, Oxford INCA Energy 350) and ultrahigh resolution scanning system (ASID-3D) in a regime of secondary electron image (SEI). The accelerating voltage is 15 kV and I ~65 A.The pressure is of the order of 10^{-4} Pa.

The electrochemical charge-discharge behavior of $Na_xNi_{0.5}Mn_{0.5}O_2$ was examined by using EL-CELL type two-electrode cells comprising Li | $LiPF_6$ (EC:DMC) |$Na_xNi_{0.5}Mn_{0.5}O_2$. The positive electrode, supported onto an aluminium foil, represented a mixture, containing 80% of the active composition $Na_xNi_{0.5}Mn_{0.5}O_2$, 7.5% C-NERGY KS 6 L graphite (TIMCAL), 7.5% Super C65 (TIMCAL) and 5% polyvinylidene fluoride (PVDF). The electrolyte contains 1M $LiPF_6$ solution in ethylene carbonate and dimethyl carbonate (1:1 by volume) with less than 20 ppm of water. Lithium electrodes consisted of a clean lithium metal disk with diameter of 15 mm. The cells were mounted in a dry box under Ar atmosphere. The electrochemical reactions were carried out using an eight-channel Arbin BT2000 system in galvanostatic mode. The test cells were galvanostatically cycled between 2.5 V and 4.5 V. The charge and discharge rates can be expressed as C/h, being h the number of hours needed for the insertion of one lithium per formula unit at the applied current intensity. All cells are cycled at a rate of C/30.

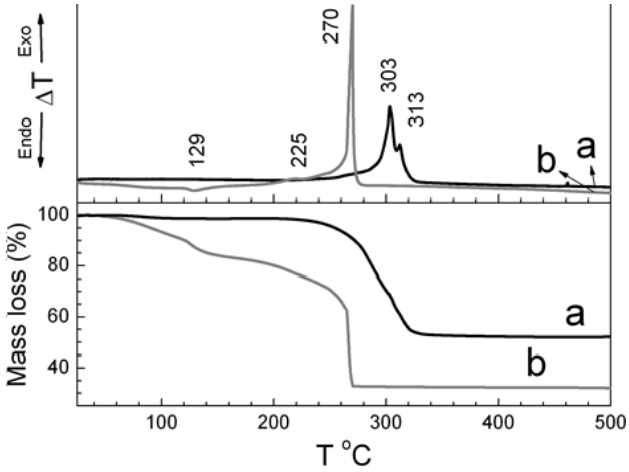

Figure 1. DTA and TGA curves for freeze-dried acetate (a) and nitrate-acetate (b) precursors.

3.RESULTS AND DISCUSSION

3.1.Structure and morphology of $Na_{0.67}Ni_{0.50}Mn_{0.50}O_2$

Freeze-drying of acetate and mixed nitrate-acetate solutions yields amorphous Na-Ni-Mn precursors. Figure 1 compares the DTA and TGA curves of two types of precursors. Acetate precursor displays one endothermic effect between 80 and 120 °C accompanied with a weight loss of 1.8% due to H_2O release. This enables to estimate the composition of acetate precursor: $Na_{0.67}Ni_{0.50}Mn_{0.50}(CH_3COO)_{2.67}.\sim 0{,}2H_2O$. Above

220 °C, there is a broad and complex exothermic peak corresponding to the decomposition of the acetate. The decomposition process is completed at 335 °C, where the weight loss reaches about 45%. In comparison with the acetate precursor, the freeze drying process for nitrate-acetate precursor is less effective. Between 80 and 165 °C, the nitrate-acetate precursor displays one endothermic effect together with a weight loss of 17% due to the release of 2.5 mole H_2O. However, the thermal decomposition of nitrate-acetate precursor is more complex process: the decomposition starts above 200 °C followed by a strong exothermic peak in a close temperature range of 260-280 °C. The total weight loss is of 51%. It is noticeable that the decomposition of nitrate-acetate precursor is completed at lower temperature in comparison with that of the acetate precursor.

At 700 °C, thermal annealing of decomposed precursors yields layered sodium nickel-manganese oxides containing impurities of the NiO-like phase. Figure 2 presents the XRD patterns of NNM-Ac and NNM-NAc. Irrespective of the type of the organic component in precursors, the XRD patterns of NNM-Ac and NNM-NAc are satisfactory fitted by the Rietveld analysis on the basis of two-phase model: layered phase (*R3m* space group) and cubic NiO phase (*Fm-3m* space group). The crystal structure of $Na_{0.67}Ni_{0.5}Mn_{0.5}O_2$ is built from $Ni_{0.5}Mn_{0.5}O_2$–layers of edge–sharing metal octahedra where the Na^+ ions are sandwiched between the layers. Based on the number of the $Ni_{0.5}Mn_{0.5}O_2$–layers in the unit cell and the Na site symmetry (i.e. prismatic), the structure of $Na_{0.67}Ni_{0.5}Mn_{0.5}O_2$ can be classified as *P3*-type. This is a general structure notation for both sodium and lithium transition metal oxides proposed by Delmas *et al.* [11]. The lattice parameters of acetate- and nitrate-derived oxides $Na_{0.67}Ni_{0.5}Mn_{0.5}O_2$ are summarized in Table 1. The comparison shows that lattice parameters are the same and they are insensitive towards the type of the organic component used in the precursors. This means that at 700 °C a stable *P*3-modification of $Na_{0.67}Ni_{0.5}Mn_{0.5}O_2$ is formed.

In addition, the amount of the NiO-related phase is less than 1%. This is consistent with previous data on limited solubility of Ni in *P3*-Na_xMnO_2 (up to 0.5 mol) [5,12,13]. It appears that the synthesis of $Na_{0.67}Ni_{0.5}Mn_{0.5}O_2$ takes place as in case of a formation of high-voltage $LiNi_{1/2}Mn_{3/2}O_4$ spinel, where the impurity NiO-like phase pursues always the target phase [14].

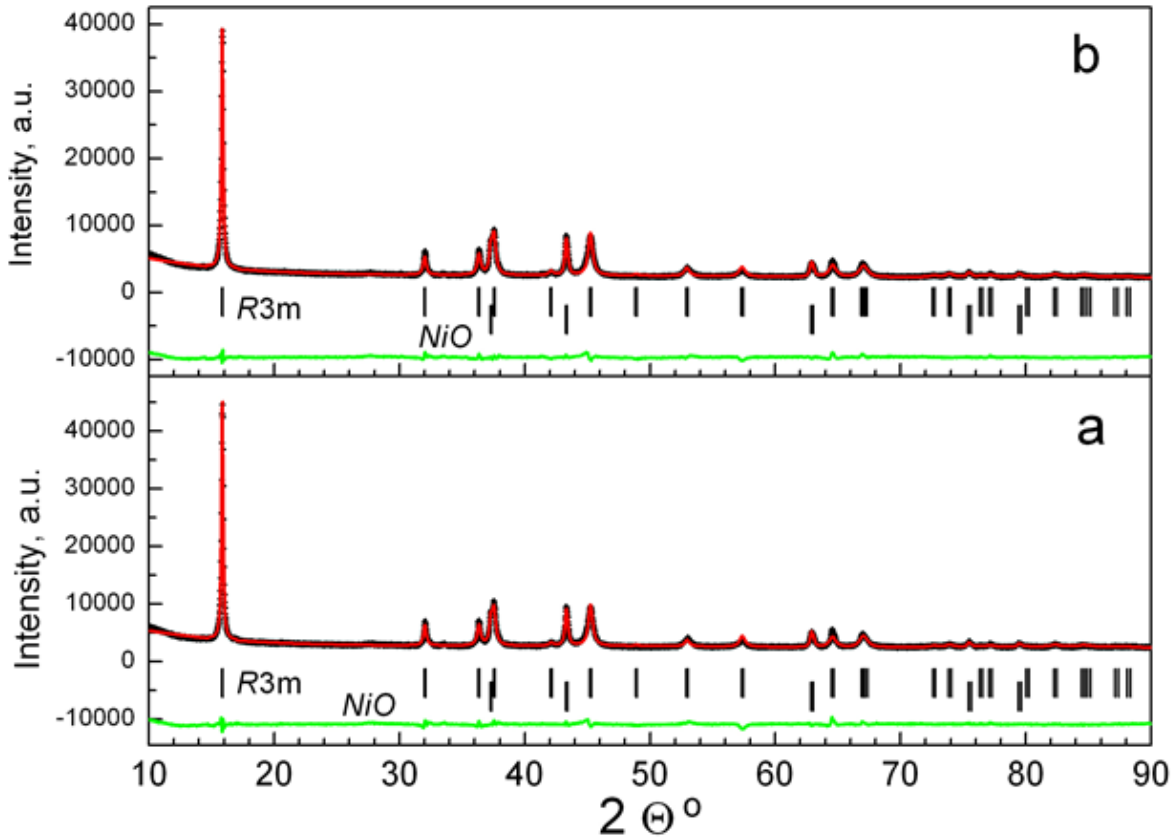

Figure 2. XRD patterns of $Na_{0.67}Ni_{0.5}Mn_{0.5}O_2$ obtained from the acetate (a) and the nitrate-acetate (b) precursors at 700 °C. The Bragg's reflections for *P3*-type structure and NiO-like phase are given. Dotted and full lines correspond to the experimental and simulated XRD patterns using Rietveld refinement. The difference between experimental and stimulated is shown below the spectra.

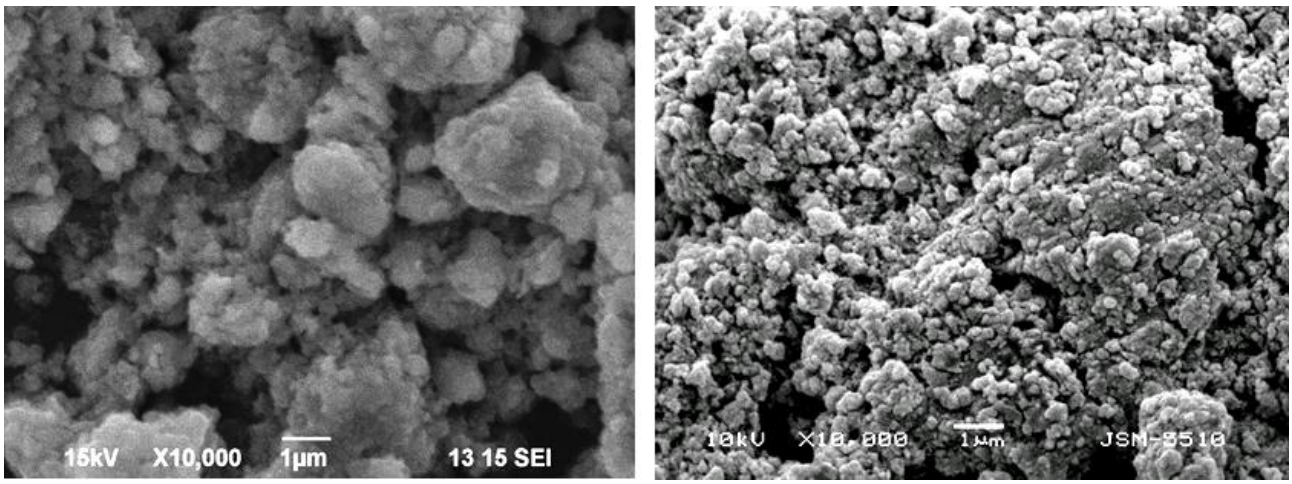

Figure 3 SEM images of $Na_{0.67}Ni_{0.5}Mn_{0.5}O_2$ obtained from the acetate (left) and the nitrate-acetate (right) precursors at 700 °C.

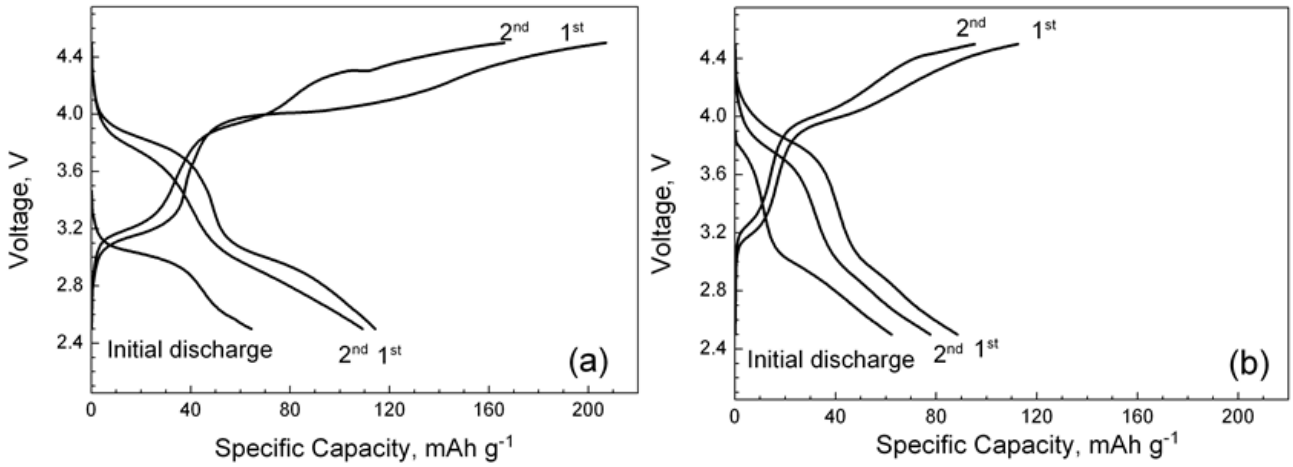

Figure 4. First and second charge/discharge curves of NNM-Ac (a) and NNM-NAc (b). All cells starts with a discharge mode, which is indicated as initial discharge.

The SEM images of acetate- and nitrate-derived oxides are compared on Figure 3. On the first glance, all oxides are composed from particles with sizes of about 100 nm that are bounded into aggregates (Fig. 3). However, close inspection of SEM images reveals a different density of aggregates. It appears that nanoparticles are loosely coupled between them when the acetate precursor is used. In the case of the nitrate-acetate precursor, all nanoparticles seem to be stick together into more dense aggregates. This can be related with the thermal properties of two types of precursors: the nitrate-acetate precursor mimics the combustion process between 240 and 280 °C due to the simultaneous presence of the nitrate ions as an oxidizer and the acetate ions as a fuel (Fig. 1). In order to create an oxidation atmosphere during the thermal decomposition of acetate precursors, an oxygen flow is used.

3.2.Electrochemical properties of $Na_{0.67}Ni_{0.50}Mn_{0.50}O_2$

Recently, we have demonstrated that *P3*-$Na_{0.67}Ni_{0.5}Mn_{0.5}O_2$ can participate in a series of reactions comprising lithium intercalation and exchange of Li^+ for Na^+ [5,6,7]. This fact, in its turn, determines the potential of *P3*-$Na_{0.67}Ni_{0.5}Mn_{0.5}O_2$ for direct use as a cathode in lithium ion batteries. In this study we are focused on the effect of the synthesis procedure on the electrochemical performance of *P3*-$Na_{0.67}Ni_{0.5}Mn_{0.5}O_2$.

Figure 4 shows the first and second charge/discharge curves for NNM-Ac and NNM-NAc. The cell starts with a discharge mode, which corresponds to a lithium intercalation in sodium deficient oxides. During the discharge, a capacity of about 65 mAh g^{-1} is obtained for both oxides (Fig. 4). This value corresponds to the intercalation of 0.3 mole Li^+ into *P3*-$Na_{0.67}Ni_{0.5}Mn_{0.5}O_2$. It is worth to mention that the content of intercalated Li^+ coincides with the amount of sodium deficiency in *P3*-$Na_{0.67}Ni_{0.5}Mn_{0.5}O_2$. The discharge profile shows a distinct plateau at 3.0 V, which is more pronounced for the acetate-derived oxide. This indicates that lithium intercalation into *P3*-$Na_{0.67}Ni_{0.5}Mn_{0.5}O_2$ is a two-phase reaction and its mechanism is not dependent on the method of

oxide synthesis. Based on HR-TEM and SAED, we have demonstrated a structure transformation from the *P3*- to the *O3*-type of structure during electrochemical intercalation of Li^+ into layered $Na_xNi_{0.5}Mn_{0.5}O_2$ at 3.04 V [7].

During the reverse process of charge, both oxides are clearly distinguished: a higher charge capacity is achieved for the oxide obtained from the acetate precursors, i.e. 207 versus 113 mAh g^{-1}, respectively (Fig. 4). These values exceed significantly the discharge capacity, thus indicating a possible participation of Na^+ in addition to Li^+ in the charge process. However, it could be taken into account that additional side reactions (such as electrode-electrolyte interactions, electrolyte decomposition, etc.) take also place above 4.4 V.

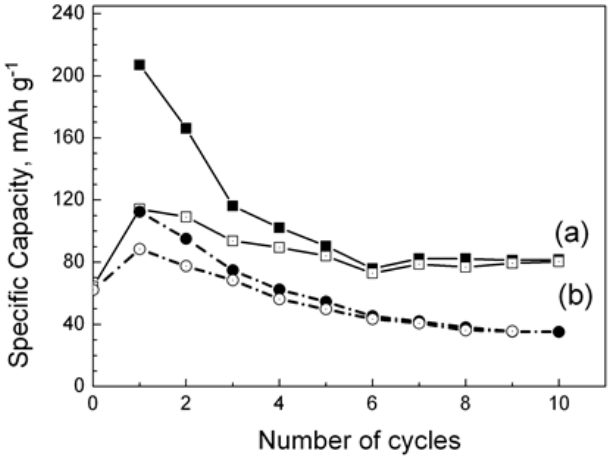

Figure 5 Cycling stability curves of of NNM-Ac (a) and NNM-NAc (b). The open and close symbols correspond to the discharge and charge capacity.

The difference in the electrochemical performances of both NNM-Ac and NNM-NAc oxides remains during the second discharge: NNM-Ac delivers a higher capacity in comparison with that for NNM-NAc, i.e. 115 versus 90 mAh/g, respectively. This means that about 0.45 and 0.35 mole of Li^+ is reinserted in NNM-Ac and NNM-NAc. The important issue is related with an irreversible capacity after the first charge and discharge. It appears that the acetate-derived oxide NNM-Ac has a higher irreversible capacity. The irreversible capacity diminishes during cycling. Figure 5 gives the cycling stability curves for NNM-Ac and NNM-NAc. After several charge/discharge cycles, a steady state performance is reached: for NNM-Ac the columbic efficiency tending to 100% is reached after 5 cycles, while after 3 cycles NNM-NAc displays columbic efficiency higher than 97%. During prolonged cycling, the reversible capacity delivered by NNM-Ac is significantly higher in comparison with that for NNM-NAc: 85 mAh g^{-1} versus 45 mAh/g, respectively.

The comparison of cycling stability curves outlines clearly that after the first irreversible capacity the electrochemical performance of acetate-derived $Na_{0.67}Ni_{0.5}Mn_{0.5}O_2$ is much better than that of the nitrate-acetate derived oxide. The huge irreversible capacity is a specific feature for NNM-Ac and can be explained if we suggest a higher reactivity of NNM-Ac towards the electrolyte leading to the formation of surface electrochemical interface (SEI). The formation of possible SEI does not interrupt the reversible lithium intercalation into NNM-Ac. The same scenario has recently been established for lithium transition metal oxides $Li_{1+x}M_{1-x}O_2$ having lithium in excess [15]. The excess of lithium is accommodated in the transition metal layers by substituting for transition metal ions. Above 4.4 V, it has been found that oxides with lithium excess undergo a structural transformation by releasing of lithium from transition metal layers in the form of Li_2O, the layered structure being preserved. It is worth to note that after this structural transformation a high reversible capacity and a good cycling stability are achieved. Contrary to lithium-excess oxides, sodium and transition metals forms only sodium deficient and sodium stoichiometric transition metal oxides. Therefore, we can suppose that the formation of SEI on sodium deficient oxides obtained from acetate precursors is most plausible phenomenon. Based on XPS analysis, we have demonstrated that, in the course of the electrochemical reaction, the oxide surface is covered with sodium and lithium phospho-fluorine-based compounds, which remain stable during the cycling [6]. This is a consequence of the reactivity of sodium deficient oxides towards $LiPF_6$ salt in the electrolyte, the reaction being intensified at potentials higher than 4.4 V [6]. The important funding of the present study is the different reactivity of oxides obtained from the acetate and nitrate-acetate precursors towards $LiPF_6$ salt in the electrolyte. It appears that SEI formed on oxides contributes to their cycling stability. Further optimization of the electrochemical properties of sodium deficient oxides are closely related with the selection of appropriate electrolyte composition.

4.CONCLUSIONS

Sodium-deficient nickel-manganese oxides $Na_{0.67}Ni_{0.5}Mn_{0.5}O_2$ with a *P3*-type of structure are obtained at 700 °C from freeze-dried acetate and nitrate-acetate precursors. The morphology of both acetate and nitrate-acetate derived oxides consists

of aggregates with micrometric dimensions, which are building from particles with nanometric dimensions. The density of aggregates shows a dependence on the type of organic component used in precursors: nanoparticles are loosely coupled between them when the acetate precursor is used, while for the oxide derived from nitrate-acetate precursor, all nanoparticles seem to be stick together into more dense aggregates.

Both acetate and nitrate-acetate derived oxides display reversible lithium intercalation when used as electrodes in model lithium cells. The better electrochemical behavior (in terms a reversible capacity and cycling stability) is observed for $Na_{0.67}Ni_{0.5}Mn_{0.5}O_2$ obtained from the acetate precursor. The good electrochemical behavior is related with a higher reactivity of acetate-derived oxides towards the electrolyte leading to the formation of SEI during the first charge to 4.5 V. The electrochemically formed SEI has a main contribution to improved cycling stability.

Acknowledgments.*This work was supported by European Social Fund (Grant BG051PO001-3.3.06-0050).*

REFERENCES

1. R. Alcántara, P. Lavela, J. L. Tirado, E. Zhecheva, R. Stoyanova, *J. Solid State Electrochem.*, **3**, 121 (1999).
2. B.L. Ellis, K.T. Lee, L.F. Nazar, *Chem. Mater.*, **22**, 691 (2010).
3. N. Nitta, F. Wu, J.T. Lee, G. Yushin, *Mater. Today*, **18**, 252 (2015).
4. X. Xu, S. Lee, S. Jeong, Y. Kim, J. Cho *Mater. Today*, **16**, 487 (2013).
5. M. Kalapsazova, R. Stoyanova and E. Zhecheva, *J. Solid State Electrochem.*, **18**, 2343 (2014).
6. M. Kalapsazova, R. Stoyanova, E. Zhecheva, G. Tyuliev, D. Nihtianova, *J. Mater. Chem. A*, **2**, 19383 (2014).
7. M. Kalapsazova, G. F. Ortiz, J. L. Tirado, O. Dolotko, E. Zhecheva, D. Nihtianova, L. Mihaylov and R. Stoyanova, *ChemPlusChem* (in press).
8. M. K. Song, S. Park, F. M. Alamgir, J. Cho, M. Liu, *Mat. Sci. Eng.* **R72**, 203 (2011).
9. Z. Gong, Y. Yang, *Energy Environ. Sci.*, **4**, 3223 (2011).
10. J. Rodrıguez-Carvajal, *Commission on Powder Diffraction Newsletter*, **26**, 12 (2001).
11. C. Delmas, C. Fouassier, P. Hagenmuller, *Phys B+C*, **91**, 81 (1980).
12. Z. Lu, R.A. Donaberger, J.R. Dahn, *Chem. Mater.*, **12**, 3583 (2000).
13. J.M. Paulsen, R. Donaberger, J.R. Dahn, *Chem. Mater.*, **12**, 2257 (2000).
14. Sv. Ivanova, E. Zhecheva, R. Stoyanova, D. Nihtianova, S. Wegner, P. Tzvetkova, Sv. Simova, *J. Phys. Chem. C*, **115**, 25170 (2011).
15. Y. Wu, C. Ma, J. Yang, Z. Li, C. Liang, L.F. Allard, M. Chi, *J. Mater. Chem. A*, **3**, 5385 (2015).

ВЛИЯНИЕ НА НАЧИНА НА СИНТЕЗ ВЪРХУ ЕЛЕКТРОХИМИЧНИТЕ СВОЙСТВА НА $Na_{2/3}Ni_{1/2}Mn_{1/2}O_2$, ИЗПОЛЗВАН КАТО ЕЛЕКТРОДЕН МАТЕРИАЛ В ЛИТИЕВО-ЙОННИ БАТЕРИИ

М. Калъпсъзова*, Р. Стоянова, Е. Жечева

Институт по обща и неорганична химия, Българска академия на науките, Ул. Акад. Г. Бончев, бл. 11, София 1113, България

Постъпила на 20 юли, 2015 г. коригирана на 23 октомври, 2015 г.

(Резюме)

В настоящата статия ние изследваме в детайли влиянието на начина на синтез върху електрохимичните свойства на $Na_xNi_{1/2}Mn_{1/2}O_2$ с x=2/3 при използването му като електрод в литиеви клетки. За получаването на оксидите $Na_{0.67}Ni_{0.5}Mn_{0.5}O_2$ е избран метода на прекурсорите. Този метод се основава на образуване на хомогенни прекурсорни фази, които лесно се превръщат в целевия продукт чрез серия от нискотемпературни реакции. Прекурсорите са получени чрез лиофилизация на водни разтвори на соли на Li(I), Ni(II) и Mn(II). Избрани са два вида разтворими соли: ацетати и нитрати. При термична обработка на лиофилизираните ацетатни-нитратни прекурсори при температури над 400 ºC се получава слоест $Na_{0.67}Ni_{0.5}Mn_{0.5}O_2$ с *P*3-тип структура. Термичните свойства на ацетатните-нитратните прекурсори са изследвани чрез DTA/TG анализ. Кристалната структура и морфологията на $Na_xNi_{1/2}Mn_{1/2}O_2$ са изследвани посредством прахова рентгенова дифракция и СЕМ анализ. Електрохимичните своиства на $Na_{0.67}Ni_{0.5}Mn_{0.5}O_2$ са изучени в моделни литиеви клетки. Оксидът $Na_{0.67}Ni_{0.5}Mn_{0.5}O_2$ получен от лиофилизирани ацетатни прекурсори показва по-добри електрохимични характеристики по отношение на обратим капацитет и стабилност при циклиране.